Energy Loss Analysis in a SiC/IGBT Propulsion Inverter over Drive Cycles Considering Blanking time, MOSFET's Reverse Conduction and the Effect

Energy Loss Analysis in a SiC/IGBT Propulsion Inverter over Drive Cycles Considering Blanking time, MOSFET's Reverse Conduction and the Effect of Thermal Feedback

Sepideh Amirpour
Department of Powertrain Engineering
China Euro Vehicle Technology AB
Gothenburg, Sweden
sepideh.amirpour@cevt.se

Torbjörn Thiringer
Department of Electrical Engineering
Chalmers University of Technology
Gothenburg, Sweden
torbjorn.thiringer@chalmers.se

Dan Hagstedt
Department of Powertrain Engineering
China Euro Vehicle Technology AB
Gothenburg, Sweden
Dan.Hagstedt@cevt.se

Abstract— **This paper presents a comparison of power and energy losses for two silicon carbide (SiC) and one silicon insulated gate bipolar transistor (Si-IGBT) power modules in a three-phase inverter, when considering the effect of blanking time and the MOSFET's reverse conduction. Two different drive cycles are chosen for the loss comparisons, the ECE-City manual and the Worldwide Harmonized Light Vehicles Test Cycle (WLTC). For the WLTC, the urban and highway phases are included. The focus of this paper is to determine the influence of the thermal feedback on the power loss calculation over the driving patterns. The analysis shows that, without accounting for the thermal feedback, the power loss levels are considerably underestimated, up to 1.5% on the conduction losses of the SiC inverters and up to 3% on the switching losses of the IGBT inverter over the ECE-City manual. Similarly, for the WLTC drive cycle, a loss increases up to 3.5% on the conduction losses of the SiC and up to 6% on the switching losses of the IGBT inverters are observed, when considering the thermal feedback. The data is derived at a chosen high torque, low speed operating point of a permanent magnet synchronous machine (PMSM) over the drive cycles. The operating point is considered as a worse operating condition from the power loss perspective.**

Keywords— Silicon Carbide (SiC), Voltage Source Inverters (VSI), MOSFET Reverse Conduction, Thermal Feedback, Energy Loss, Electric Vehicle

I. INTRODUCTION

New generations of commercial Wide Band Gap silicon carbide (SiC) MOSFETs seem to be a promising alternative compared to commonly used silicon insulated gate bipolar transistors (Si-IGBTs) in hybrid powertrains and electrified vehicle applications [1], [2]. Lower switching losses due to faster switching transitions, combined with better thermal characteristics make these attractive to Si-IGBTs. In addition, lower conduction losses can be achieved by the MOSFET's reverse conduction phenomenon. Combined with an optimal control strategy for the drive system [9], the overall efficiency of the powertrain can be improved, which results in a lighter cooling system, higher power density, increased range, etc. Several researches have compared the SiC-MOSFETs and traditional Si-IGBTs for EV-applications with respect to the MOSFET's reverse conduction, energy efficiency as well as the energy losses for different drive cycles [1]–[3]. However, to the author's knowledge, there is a lack of comprehensive comparisons which numerically quantifies the effect of considering and neglecting the thermal feedback on the power loss calculations over different drive cycles while covering the impacts of blanking time and MOSFET's reverse conduction.

The purpose of this paper is to compare the power and energy losses, with and without the effect of thermal feedback of a recently introduced 3rd generation half-bridge SiC module, CAB450M12XM3 and the 2nd generation, CAS300M12BM2 in the 1200V class with a 1200V Si-IGBT, FZ600R12KE3 for the relevant operating points of a permanent magnet synchronous machine (PMSM). The total power and energy losses of the propulsion inverter for the three modules are derived by implementing space vector modulation (SVM) and making a comparison for the two different driving patterns. Fig. 1, illustrates an overview of the analysis.

II. REVERCE CONDUCTION AND BLANKING TIME

A major difference of the investigated modules is their current conduction behavior. In Si-IGBTs the total reverse current of the transistor flows through an anti-parallel diode, while MOSFETs can also conduct in the opposite direction through their reverse conduction characteristic. In the inverter, either the upper or the lower diode in one leg is conducting when the current and voltage have different signs in the same phase leg. Therefore, if the corresponding MOSFET's drain to source voltage gets higher than the diode's threshold voltage, parallel conduction of the two devices occurs. The diode can either be a separate diode or the intrinsic inbuilt one. This capability influences the conduction losses distribution in SiC-MOSFETs, resulting in reduced power losses.

To avoid a shoot through fault in a pulse width modulation (PWM) controlled inverter, a blanking time is introduced, where both the upper and lower switches in the same phase leg are off and only the diode is conducting during this time. Therefore, the total conduction loss of the modules is influenced by the diode conduction during the blanking time.

III. CONDUCTION LOSSES INCLUDING BLANKING TIME AND MOSFET'S REVERSE CONDUCTION

A. Conduction Losses in the SiC Power Module

In this study, the conduction losses for a three-phase

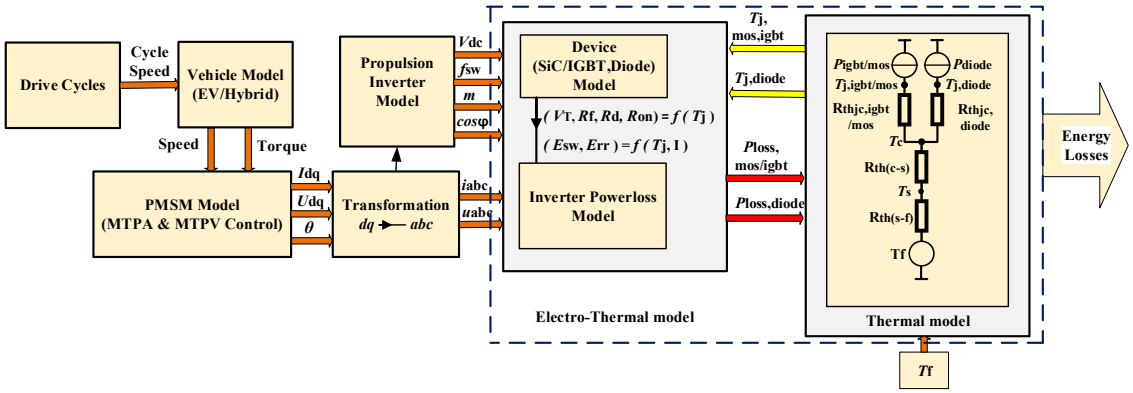

Fig. 1. System simulation model overview.

voltage source inverter are determined numerically using MATLAB. The used numerical implementation is based on an analytical approach for SiC-MOSFETs' conduction losses which is presented in [4], [5]. In this approach, the average MOSFET conduction losses over a fundamental period of the phase current can be calculated as

$$P_{cond,MOS} = \frac{1}{2\pi}\int_0^{2\pi} R_{on} I_M^2(\alpha)\tau(\alpha)\, d\alpha \quad (1)$$

where R_{on} is the MOSFET on-state resistance, I_M is the MOSFET current, $\alpha = 2\pi f t$ where f is the fundamental frequency and τ is the duty cycle which can be expressed as a function of α as

$$\tau(\alpha) = \frac{1}{2}(1 + m\sin\alpha) \quad (2)$$

where m is the modulation index [6]. Likewise, the diode conduction losses can be derived as

$$P_{cond,D} = \frac{1}{2\pi}\int_0^{2\pi} (R_d I_D^2(\alpha) + V_d I_D(\alpha))\tau(\alpha)\, d\alpha \quad (3)$$

where the voltage drop, V_d, and the on-state resistance, R_d, can be obtained from the datasheet information of the forward characteristics of the diode, I_D is the diode current.

During reverse conduction, the MOSFET and diode's current can be obtained as,

$$I_M = \frac{R_d I_p \sin(\alpha-\varphi) - V_d}{R_d + R_{on}} \quad (4)$$

$$I_D = \frac{R_{on} I_p \sin(\alpha-\varphi) + V_d}{R_d + R_{on}} \quad (5)$$

where φ is the angle of displacement power factor and I_p is the peak phase current [4].

In Fig. 2 the losses with and without the MOSFET reverse conduction are presented for the upper diode and MOSFET in a phase leg of CAS300, SiC inverter. A significant reduction in the diodes' total conduction losses up to 96%, is observed as the result of parallel conduction. Likewise, for the CAB450 inverter, a reduction up to 97% in diodes' conduction losses is noticed. The operating condition used for calculating the losses is presented in Table. I, which is an

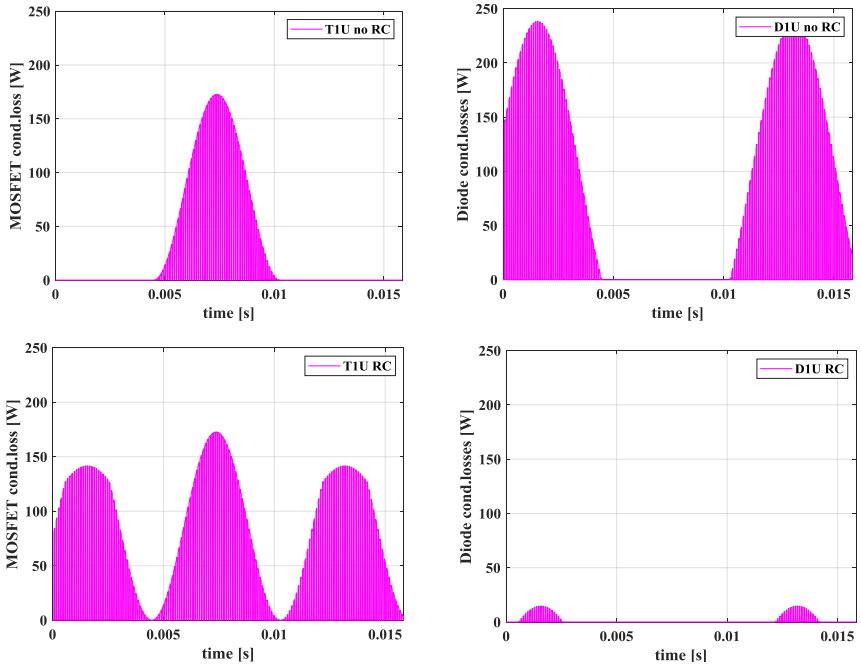

Fig. 2. MOSFET and Diode conduction losses with and without MOSFET reverse conduction (RC) in CAS300, SiC inverter, upper MOSFET and Diode in a phase leg.

TABLE I. CHOSEN OPERATING POINT OVER WLTC AND ECE-CITY MANUALL FOR THE LOSSES COMPARISON

Variable	WLTC	ECE-City
Current magnitude [A]	272	178
DC voltage [V]	300	300
Blanking time [µs]	0.5	0.5
Switching Frequency [kHz]	10	10
Torque [Nm]	89	57
Mechanical speed [rpm]	1290	1326

operating point of the used PMSM, at high current magnitude, corresponding to high torque and low speed of the WLTC drive cycle.

B. Conduction Losses in the IGBT Power Module

The conduction losses of a Si-IGBT and diode in a Si-IGBT module can be calculated by integrating the product of the current flowing through the device and voltage drop over it [7], [8], resulting in the expressions as

$$P_{cond,IGBT} = \frac{1}{2}\left(V_T\frac{I_p}{\pi} + R_f\frac{I_p^2}{4}\right) + m\cos\varphi\left(V_T\frac{I_p}{8} + \frac{1}{3\pi}R_f I_p^2\right) \quad (6)$$

$$P_{cond,Diode} = \frac{1}{2}\left(V_d\frac{I_p}{\pi} + R_d\frac{I_p^2}{4}\right) - m\cos\varphi\left(V_d\frac{I_p}{8} + \frac{1}{3\pi}R_d I_p^2\right) \quad (7)$$

where R_f is the IGBT on-state resistance and V_T is the IGBT voltage drop.

C. Blanking Time

In order to include the effect of the blanking time in the conduction power losses calculation, an equivalent duty cycle to be used in the mentioned conduction loss equations, can be introduced as,

$$\tau_{eq}(\alpha) = \tau(\alpha) - t_{blanking}f_{sw} = \frac{1}{2}(1 - 2t_{blanking}f_{sw} + msin\alpha) \quad (8)$$

where f_{sw} is the switching frequency [4].

Fig. 3 shows the diode and MOSFET currents in a phase leg of the CAS300 inverter, without (upper one) and with (lower one) the effect of blanking time, when also considering the MOSFET reverse conduction. As shown in the lower figure, during the blanking time, only the diode is conducting the current. This leads to an increase of up to 8 W on the diodes' conduction losses for the CAS300 inverter, when considering the MOSFET reverse conduction. The effect on the MOSFETs' conduction losses is small and then ignored. For CAB450 and FZ600, an increase of up to 33 W and 4.5 W, on the diodes' conduction losses is noticed, respectively. Fig.4 illustrates the upper diode conduction losses in a phase leg of CAS300, without and with blanking time, when the MOSFET reverse conduction is also considered. The operating condition used for calculating the diodes' conduction losses, is presented in Table. I.

IV. SWITCHING LOSSES IN IGBT AND SIC MOSFET

During every turn on and turn off event, a loss occurs in the switch and its anti-parallel/body-diode. The switching

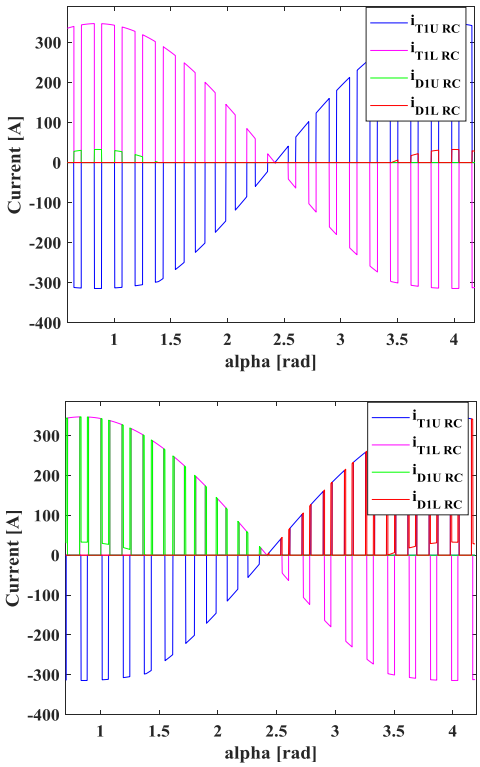

Fig. 3. Impact of blanking time on diode and MOSFET currents as function of $\alpha = 2\pi ft$ with considering the MOSFET's reverse conduction in a phase leg of CAS300 inverter. Upper figure with no blanking time, lower figure with blanking time.

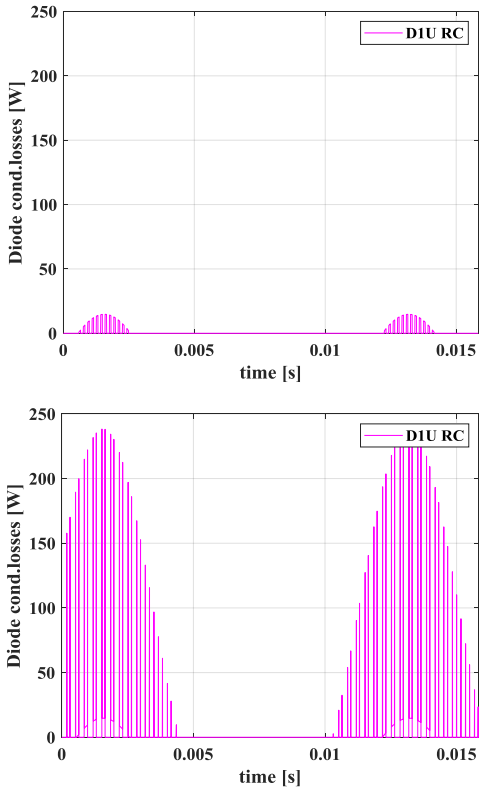

Fig. 4. Diode conduction loss, no blanking time (top), with blanking time (bottom) in a phase leg of CAS300 inverter.

energy of the Si-IGBTs and diodes are generally higher than those of the SiC devices. Switching losses can be calculated in an IGBT, MOSFET and diode analytically by the expression as

$$P_{sw.MOSFET,IGBT,Diode} = f_{sw} \cdot E_{sw(@I_{nom},V_{nom})} \cdot (\frac{1}{\pi}\frac{I_p}{I_{nom}})^{k_i} . (\frac{V_{dc}}{V_{nom}})^{k_v} \quad (9)$$

where E_{sw} is switching energy loss, I_p is the peak phase current, I_{nom} and V_{nom} are nominal current and voltage values and k_i , k_v are current and voltage dependency exponents, respectively [8]. In the numerical implementation in this study, the switching loss is calculated at every switch-on and switch-off event of the device as

$$P_{sw} = \frac{\sum E_{sw}}{t} \quad (10)$$

where t is the total simulation time.

V. THERMAL CALCULATION MODEL

As some parameters in the power modules, such as on-state resistances, forward voltage drops, switching and reverse recovery energies are temperature-dependent, the inverters' power losses are found by using a thermal network which is presented in Fig. 5 for the compared modules. T_j, represents the junction temperatures of the MOSFET/IGBTs and diodes, T_c is the case temperature, T_s and T_f represent the heatsink and fluid temperatures, respectively. For a fair comparison, the same heatsink is used for each inverter. It is worth to note that, for the SiC-based inverters, three SiC half-bridge modules are used and for the IGBT-based inverter, six IGBT modules are used. All set-ups are normalized to the same current rating level of 600 A. The fluid temperature is set to 65 ℃ and the flow rate to 10 L/min. The CAB450 module is using the latest 3rd GEN MOSFET dies which have an inbuilt body diode, hence the module does not have an antiparallel diode, compared to CAS300 which has an additional antiparallel Schottky diode with zero reverse recovery energy.

VI. COMPARISON OF LOSSES IN THREE PHASE SIC/IGBT INVERTERS WITH AND WITHOUT THERMAL FEEDBACK

To compare the power losses of the three investigated modules, an operating point of a PMSM at high current magnitude is used, corresponding to high torque and low speed of the two drive cycles. The chosen operating point can be considered as a worse operating condition in the urban driving cycles from the power loss point of view. The PMSM is controlled by implementing a control strategy comprising of Maximum Torque per Ampere (MTPA) and Maximum Torque per Volt (MTPV) control. Under this control strategy, the PMSM operates in constant torque range as well as in the partial and full field weakening ranges [9], [10]. The chosen operating point is shown in Table. I for both the driving cycles and the vehicle model parameters are given in Table. II.

TABLE II. VEHICLE MODEL

Vehicle Parameter	Value
Total mass of the vehicle [kg]	1700
Aerodynamic drag coefficient [-]	0.7
Vehicle cross section area [m^2]	2
Rolling friction coefficient [-]	0.007
Wheel radius [m]	0.3

The losses are calculated based on the temperature in each driving cycle through an iterative approach in which, all the static and dynamic parameters of the devices are interpolated based on the junction temperature, then the losses and the temperatures are redetermined sequentially and iteratively until convergence. It can be noted that, the current dependency of the devices' switching energies is considered by interpolating the switching energies as function of current as well as the junction temperature. The results of the investigations are presented in Tables. III and IV for the SiC modules and Si-IGBT, respectively. Worth mentioning is that, in order to have the same nominal current of 600 A for the three compared modules, a scale factor is applied on the power losses of the SiC modules for a fair comparison.

According to the simulated values shown in Tables. III and IV, a significant decrease in diode conduction losses can be observed for the two SiC modules compared to the Si-IGBT module in each driving cycle. This can be explained as a result of the MOSFET's reverse conduction capability where the current between the diode and the MOSFET is shared. Moreover, from the thermal point of view, for the SiC-MOSFETs, the rate of increase of the conduction losses with respect to junction temperature is relatively high when compared to that of a Si-IGBT. The reason is a lower increase in the IGBT dynamic on-state resistance with an increase of

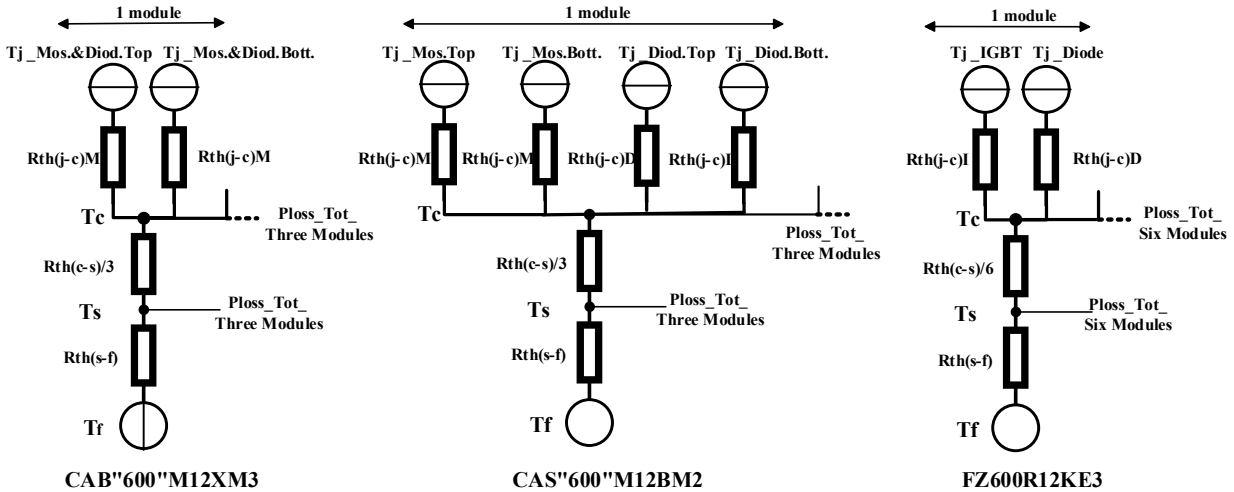

Fig. 5. Thermal calculation model to find the power losses and temperatures.

TABLE III. SIMULATED AVERAGE VALUE OF CONDUCTION AND SWITCHING LOSSES OF THE SIC INVERTER FOR TWO DRIVE CYCLES, WITH AND WITHOUT THERMAL FEEDBACK, CONSIDERING BLANKING TIME AND USING THE MOSFET'S REVERSE CONDUCTION.

CAB "600"M12XM3							
	Cond. [W]	Cond. Thermal Feedback [W]	Diff.%	Sw. [W]	Sw. Thermal Feedback [W]	Diff. %	Tjunc. Thermal Feedback [°C]
MOS's ECE/**WLTC**	97.3/**226.4**	98.5/**233.2**	1.2/**3.0**	17.9/**42.0**	17.9/**42.0**	0/**0**	68.4/**75.7**
Diodes ECE /**WLTC**	20.8/**32.8**	20.8/**32.6**	0/**-0.6**	1.1/**1.7**	1.1/**1.7**	0/**0**	68.4/**75.7**
Inver. ECE /**WLTC**	118.1/**259.2**	119.3/**265.8**	1.0/**2.5**	19.0/**43.7**	19.0/**43.7**	0/**0**	
CAS "600"M12BM2							
	Cond. [W]	Cond. Thermal Feedback [W]	Diff.%	Sw. [W]	Sw. Thermal Feedback [W]	Diff. %	Tjunc. Thermal Feedback [°C]
MOS's ECE /**WLTC**	135.2/**314.8**	137.3/**326.0**	1.5/**3.6**	21.0/**45.0**	21.0/**45.0**	0/**0**	68.3/**73.0**
Diodes ECE /**WLTC**	4.3/**7.2**	4.3/**7.3**	0/**1.4**	0/**0**	0/**0**	0/**0**	67.3/**70.5**
Inver. ECE /**WLTC**	139.5/**322.0**	141.6/**333.3**	1.5/**3.5**	21.0/**45.0**	21.0/**45.0**	0/**0**	

TABLE IV. SIMULATED AVERAGE VALUE OF CONDUCTION AND SWITCHING LOSSES OF THE IGBT INVERTER FOR TWO DRIVE CYCLES, WITH AND WITHOUT THERMAL FEEDBACK, CONSIDERING BLANKING TIME.

FZ600R12KE3							
	Cond. [W]	Cond. Thermal Feedback [W]	Diff.%	Sw. [W]	Sw. Thermal Feedback [W]	Diff.%	Tjunc. Thermal Feedback [°C]
IGBTs ECE/**WLTC**	201.5/**341.0**	202.0/**343.6**	0.25/**0.76**	85.6/**182.8**	87.6/**190.7**	2.3/**4.3**	70.5/**74.8**
Diodes ECE /**WLTC**	147.4/**242.3**	145.8/**238.5**	-1.1/**-1.6**	74.5/**141.0**	77.6/**151.4**	4.2/**7.4**	71.6/**76.4**
Inver. ECE /**WLTC**	348.9/**583.3**	347.8/**582.1**	-0.3/**-0.2**	160.1/**323.8**	165.2/**342**	3.2/**5.7**	

junction temperature. However, higher switching losses in the Si-IGBT is observed substantially, which is limiting its usability for high frequency applications. In addition, the increment of IGBT switching losses with respect to an increase in temperature is relatively high compared to its conduction losses. In SiC-MOSFETs, the effect of a temperature increase on the switching losses is almost zero for the two driving cycles. In addition, in the SiC modules, the increase rate of conduction losses in the diodes (body diode or possible external diode) with respect to an increase in junction temperature is much lower compared to that in the channel of the MOSFETs. This is due to a lower increase in the diode dynamic resistance with the temperature compared to the MOSFET's on-state resistance. Therefore, as can be seen in Fig. 6, when the junction temperature is increasing to its maximum of 150 °C, the share of current in the MOSFETs' channels is decreasing up to an amount of 100 A, compared to that of the diodes, in which the current is increasing. Moreover, a negative temperature coefficient of the diodes' voltage drop also affects on the current distribution in the SiC-MOSFET modules. Fig. 6, depicts the upper and lower MOSFET and diodes' currents in a phase leg of the CAS"600" inverter at the chosen operating point over the WLTC drive cycle. The left side figure shows the currents at 65 °C and the right one demonstrates the currents at junction temperature of 150 °C.

All in all, according to the tables above, at the chosen operating points, high torque and low speed, which are in the urban driving phases, it is shown that, in the ECE-City-manual, the total power loss of the FZ600 inverter is 374.6W and 350.3W higher than that of the CAB"600" and CAS"600" inverters, respectively. Likewise, for the WLTC drive pattern, the total loss of the FZ600 inverter is 614.7W and 545.9W higher than that of the CAB"600" and CAS"600" inverters, respectively. As expected, the total inverters' losses in the WLTC is higher than those of the ECE-City-manual cycle, due to more aggressive acceleration and decelerations which induce more thermal stress on the devices.

Moreover, the impact of the thermal feedback on the inverters' total losses is, an increase up to 1.5% and 3% for the SiCs' conduction losses and IGBTs' switching losses, respectively, at the chosen operating condition, for ECE-City manual. Similarly, a loss increases up to 3.5% on the conduction losses of the SiC and up to 6% on the switching losses of the IGBT inverters are observed for the WLTC driving schedule.

VII. INVERTERS' TOTAL ENERGY LOSS ANALYSIS FOR THE TWO DRIVE CYCLES WITH AND WITHOUT THERMAL FEEDBACK

In Figs. 7 and 8, the used driving schedules and the total energy losses for the period of 15 years (lifetime of the

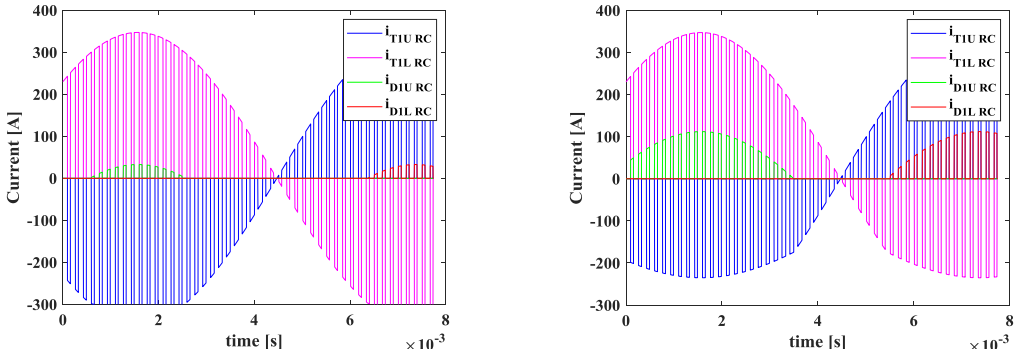

Fig. 6. MOSFET and diode currents in a phase leg of CAS"600" inverter at the chosen operating point over WLTC at the junction temperature of 65 ℃(left), and 150 ℃(right).

vehicle), 1-hour driving a day, for the three compared modules of the propulsion inverter are presented. The data is derived over the mentioned two driving patterns, after the thermal feedback is applied to all the operating points as well as when the blanking time and the MOSFET's reverse conduction are also considered.

As shown in Fig. 8, the two SiC inverters offer up to 4 and 3.5 times lower total energy losses in 15 years over the WLTC and City-manual patterns, respectively, when compared to those of the Si-IGBT inverter. This is due to lower switching losses of SiC-MOSFETs as well as lower total conduction losses.

Moreover, the energy loss differences before and after of applying the thermal feedback are calculated and compared for the three inverters in the loss difference figures in Fig. 9. With the effect of thermal feedback, for the FZ600 inverter, higher loss increases, up to 3 kWh and more than 4 kWh are observed, over ECE-City manual and WLTC, respectively. While in SiC inverters, a loss increase in the range of 1-3 kWh is observed over the two driving patterns and the effect on the SiC diodes is almost zero.

VIII. CONCLUSION

This paper presents an evaluation of the propulsion inverter losses over the two different driving patterns, comparing the Si-IGBT and the two SiC inverters. The investigation is considering, as well as neglecting, the effect of the thermal feedback on the power loss calculation. For the Si-IGBTs the total switching loss increment with respect to the temperature is more rapid compared to the conduction

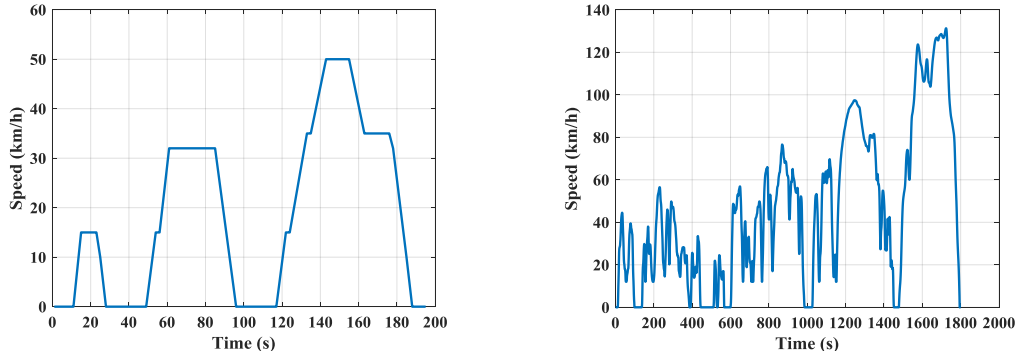

Fig. 7. ECE-City-manual driving schedule (left), WLTC driving schedule (right).

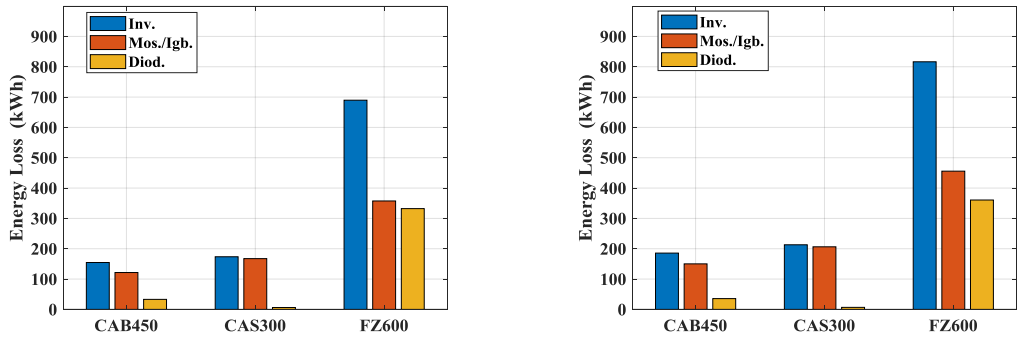

Fig. 8. Energy loss in 15 years, 1-hour driving a day, in the three modules' propulsion inverters, MOSFETs /IGBTs and diodes with thermal feedback, ECE-City-manual driving schedule (left), WLTC driving schedule (right).

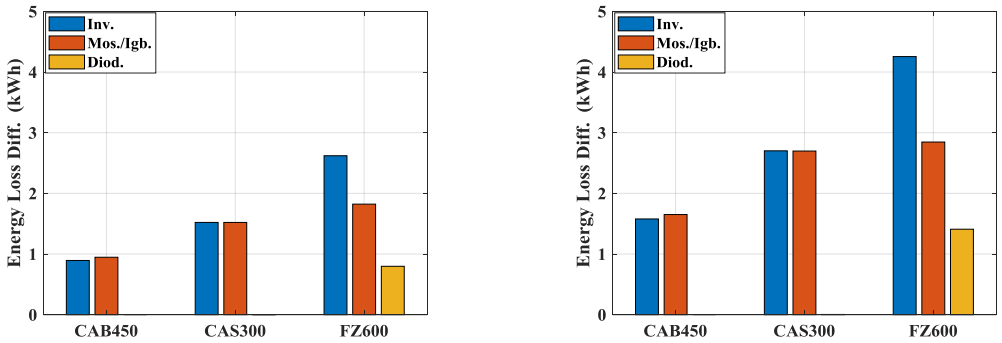

Fig. 9. Energy loss difference between thermal and no thermal effect, in 15 years, 1-hour driving a day, in the three modules' propulsion inverters, MOSFETs /IGBTs and diodes, ECE-City-manual driving schedule (left), WLTC driving schedule (right).

loss especially in WLTC. In SiC-MOSFETs the conduction losses are increasing more rapidly with the junction temperature increase. The SiC inverters show considerably lower energy losses, up to 4 times, for both the two driving cycles which make them a superior solution at higher switching frequency, even at the worst case with high torque and low speed, using the benefit of their MOSFET's reverse conduction.

ACKNOWLEDGMENT

The financial support given by the national energy administration, Energimyndigheten, as well as CEVT is gratefully acknowledged.

REFERENCES

[1] K. Kumar, M. Bertoluzzo and G. Buja, "Impact of SiC MOSFET traction inverters on compact-class electric car range," IEEE PEDES 2014.

[2] J. Biela, M. Schweizer, S. Waffler and J.W. Kolar, "SiC versus Si-Evaluation of Potentials for Performance Improvement of Inverter and DC–DC Converter Systems by SiC Power Semiconductors," IEEE Transactions on Industrial Electronics, vol. 58, , no 7, Clarendon, July 2011.

[3] R. Menon, N.A. Azeez, A.H. Kadam, and Sheldon S. Williamson, "Energy Loss Analysis of Traction Inverter Drive for Different PWM Techniques and Drive Cycles," IEEE 2018

[4] A. Acquaviva and T. Thiringer, "Energy efficiency of a SiC MOSFET propulsion inverter accounting for the MOSFET's reverse conduction and the blanking time," EPE 2017 ECCE Europe.

[5] J. Rabkowski and T. Platek, "Comparison of the power losses in 1700V Si IGBT and SiC MOSFET modules including reverse conduction," EPE'15 ECCE-Europe.

[6] J. W. Kolar, H. Ertl and F. C. Zach, "Influence of the modulation method on the conduction and switching losses of a PWM converter system," IEEE Transactions on Industry Applications, vol. 21, no 6, 1991, pp 1063-1075.

[7] F. Casanellas, "Losses in PWM inverters using IGBTs," IEEE Proc.-Electr. Power Appl., vol.141, no 5, pp.235-239.

[8] SEMIKRON, Application Manual Power Semiconductors, ISLE Verlag 2015, Ilmenau, ISBN 978-3-938843-83-3, pp. 274-279.

[9] M. Meyer and J. Böcker, "Optimum Control for Interior Permanent Magnet Synchronous Motors (IPMSM) in Constant Torque and Flux Weakening Range," EPE-PEMC 2006, pp. 282-286.

[10] M. Meyer, T. Grote and J. Böcker, "Direct Torque Control for Interior Permanent Magnet Synchronous Motors with Respect to Optimal Efficiency," EPE 2007.